User Guide to the RAPID Measurements in the Cluster Active Archive (CAA)

prepared by
Patrick W. Daly and Elena A. Kronberg

Version 3.0

Table of Contents

Reference Documents 3

List of Acronyms 3

1 Introduction 4

2 Instrument Description 4
2.1 The IES Instrument . . . 4
2.2 The IIMS Instrument . . . 4
2.3 Spin Sectorization . . . 7

3 Instrument Operations 8
3.1 Telemetry modes . . . 8
3.2 Operations on IES (electrons) . . . 8
3.3 Operations on IIMS (ions) . . . 9

4 Measurement Calibration and Processing procedures 11
4.1 Electrons . . . 11
4.2 Ions . . . 11
4.3 Standardized Energy Channels . . . 12
4.4 Phase Space Density Conversion . . . 14

5 Key Science Measurements and Datasets 14
5.1 Particle Distribution . . . 14
5.2 Auxiliary . . . 18
5.3 Status . . . 18
5.4 Graphical . . . 19
5.5 Dataset Version . . . 19
5.6 Quality flag . . . 21

6 Recommendations 21
6.1 Usability issues . . . 21

A Summary of RAPID Datasets at CAA 24

B Partial moments 26
B.1 Density . . . 26
B.2 Velocity . . . 26
B.3 Pressure . . . 27

C Phase Space Density Conversion Factors 28

D RAPID to GSE Rotation Matrix 29
D.1 The RAPID Spacecraft Frame . . . 29
D.2 The Rotation Matrix . . . 29
D.3 Example . . . 30
D.4 Things to Note . . . 31

Reference Documents

RAP-GSE: Daly, P. W. [2004]. Converting from RAPID Coordinates to GSE. *RAPID Report DS–RAP–TN–0019, Issue 1.1*, Max-Planck-Institut für Sonnensystemforschung, Katlenburg-Lindau, Germany. http://www.mps.mpg.de/dokumente/projekte/cluster/rapid/rap_to_gse.pdf.

RAP-ICD: Daly, P. W., Mühlbachler, S., and Kronberg, E. A. [2011]. Cluster Active Archive: Interface Control Document for RAPID. *Report CAA–RAP–ICD–0001, Issue 4.0*, Max-Planck-Institut für Sonnensystemforschung. http://www.mps.mpg.de/dokumente/projekte/cluster/rapid/rap_caa_icd.pdf.

Hapgood, M. A. [1992]. Space Physics Coordinate Transformations: A User Guide. *Planet. Space Sci.*, **40**, 711–717.

RAP-CR: Kronberg, E. E. and Daly, P. W. [2011]. Calibration Report of the RAPID Measurements in the Cluster Active Archive (CAA). *RAPID Report CAA–EST–CR–RAP, Issue 2.0*, Max-Planck-Institut für Sonnensystemforschung, Katlenburg-Lindau, Germany. http://www.mps.mpg.de/dokumente/projekte/cluster/rapid/caa_rap_cal.pdf.

RAP-FOM: [2000]. RAPID Flight Operations User Manual. *Version 3.0*, Max-Planck-Institut für Aeronomie, Katlenburg-Lindau, Germany. http://www.mps.mpg.de/dokumente/projekte/cluster/rapid/Rapid_flight_man30.pdf.

Wilken, B., Axford, W. I., Daly, P., Daglis, I., Güttler, W., Ip, W. H., Korth, A., Kremser, G., Livi, S., Vasyliunas, V. M., Woch, J., Baker, D., Belian, R. D., Blake, J. B., Fennell, J. F., Lyons, L. R., Borg, H., Fritz, T. A., Gliem, F., Rathje, R., Grande, M., Hall, D., Kecskeméty, K., Mckenna-Lawlor, S., Mursula, K., Tanskanen, P., Pu, Z., Sandahl, I., Sarris, E. T., Scholer, M., Schulz, M., Sørass, F., and Ullaland, S. [1997]. RAPID: The Imaging Energetic Particle Spectrometer on Cluster. *Space Science Reviews*, **79**, 399–473.

Wilken, B. et al. [2001]. First Results from the RAPID Imaging Energetic Particle Spectrometer on board Cluster. *Ann. Geophys.*, **19**, 1355–1366.

List of Acronyms

BM	Burst Mode, Cluster high telemetry rate
CAA	Cluster Active Archive
CEF	Cluster Exchange Format (CAA format)
CR	Calibration Report
DPU	Digital Processing Unit
EDB	Experiment Data Block
GEI	Geocentric Equatorial Inertial coordinate system
GSE	Geocentric Solar Ecliptic coordinate system
ICD	Interface Control Document
IES	Imaging Electron Spectrometer (part of RAPID)
IIMS	Imaging Ion Mass Spectrometer (part of RAPID)
MCP	Multichannel Plate
NM	Nominal Mode, Cluster low telemetry rate
RAPID	Research with Adaptive Particle Imaging Detectors (Cluster Experiment)
SCENIC	Spectroscopic Camera for Electrons, Neutral, and Ion Composition (part of RAPID)
TOF	Time-Of-Flight

1 Introduction

The RAPID experiment (*Research with Adaptive Particle Imaging Detectors*) on board Cluster measures 3-D energetic electron and ion fluxes in the energy range above ∼30 keV. Since the raw data delivered by the instrument are of no use without detailed knowledge of their construction, functioning, calibrations, and limitations, it is essential that the RAPID Team process this initial data set into more usable format showing physical parameters in physical units, and make them available to the scientific community. The RAPID team delivers about 50 different data products per spacecraft for each day of observations.

This User's Guide explains how to exploit the CAA RAPID dataset, how to select the right products for various applications, as well as which problems might be encountered, and what the user must watch out for.

It is intended to be concise and uncomplicated; therefore only the main products will be discussed here. A complete description of the RAPID CAA data products is given in the RAPID Interface Control Document [RAP-ICD] and the data quality issues are described in the RAPID Calibration Report [RAP-CR].

- For emphasis, important caveats are bulleted and placed inside a gray-shaded box.

2 Instrument Description

The RAPID experiment is described in *Wilken et al.* [1997] as well as in the Flight Operational Manual [RAP-FOM]. The first results are presented in *Wilken et al.* [2001].

The RAPID instrument uses two different and independent detector systems for the detection of nuclei and electrons: The **I**maging **I**on **M**ass **S**pectrometer (IIMS) and the **I**maging **E**lectron **S**pectrometer (IES).

2.1 The IES Instrument

One of the three IES detector heads is shown in the left side of Figure 1. Each functions as a pin-hole camera, with 3 microstrip detectors to locate the incoming particles to within 20°. Not shown is a foil between the pin-hole aperture and detectors that removes any ions up to 350 keV.

A single head covers an acceptance angle of 60° in all; a total of three heads span the entire range of 180° with 9 "pixels" (middle of Figure 2) in one half-plane. During one spacecraft spin (∼4 s), this plane rotate through 360°, during which time, 16 measurements are made; one speaks of 16 spin sectors which are synchronized to the sun (right side of Figure 2). A 3-D distribution thus consists of 9 polar × 16 azimuth directions.

The 3rd dimension, energy, is determined by the charge deposited in the detector by the absorbed electron, which is proportional to that energy (minus a constant). The accumulated charge is swept out and converted to a digital signal at regular intervals. Because of background currents, 0 energy corresponds to some finite signal, called the *pedestal*; 8 energy channels are defined in terms of the 256 bin numbers, relative to the expected location of this pedestal (Figure 3); see Table 1for the measured energies.

2.2 The IIMS Instrument

A single ion detector head is illustrated on the right side of Figure 1; there are three ion heads in total. The entering particle first traverses collimating plates, penetrates a thin foil that emits electrons to generate a start signal, and then strikes the solid state detector, where electrons emitted at the surface produce a stop signal. The particle energy is deposited in the detector and is recorded.

Table 1: The standardized RAPID energy channels

Channel	Hydrogen	Helium	CNO	Electrons	
				BM	NM
1	27.7–64.4[a]	*(29.9)*[b]	*(83.8)*[c]	40.7[d]	40.7[d]
2	75.3	137.8	274.4	50.5	50.5
3	92.2	172.3	414.	68.1	68.1
4	159.7	235.1	498.	94.5	94.5
5	374.	351.	638.	127.5	127.5
6	962.	737.	948.	175.9	244.1
7	1885.	1689.	1414.	244.1	—
8	—[e]	—[e]	2539.	336.5	—
Upper	4007.	3799.	4046.	406.5	406.5

Lower thresholds, all units keV

[a] Energy gap between hydrogen 1 & 2
[b] Helium channel 1 contains hydrogen, suppressed
[c] CNO channel 1 contaminated at times, suppressed
[d] Temporary pseudo value, see RAP-CR
[e] 8th channel not accessible for hydrogen and helium

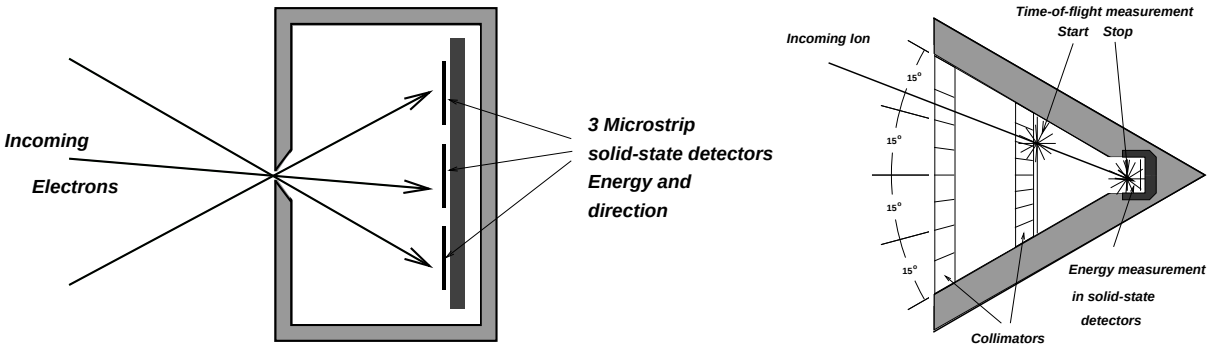

Figure 1: Left: One of the three IES heads, containing three solid state detectors to determine the direction of the incoming detected electron to within 20°. Right: One of the three SCENIC heads making up the IIMS part of RAPID. Shown is an incoming ion that triggers a start signal at a foil, which also serves to determine the fine direction, and a stop signal when it enters the solid state detector, where its energy is measured. The stop and start signals are detected by multichannel plates (MCPs), not shown.

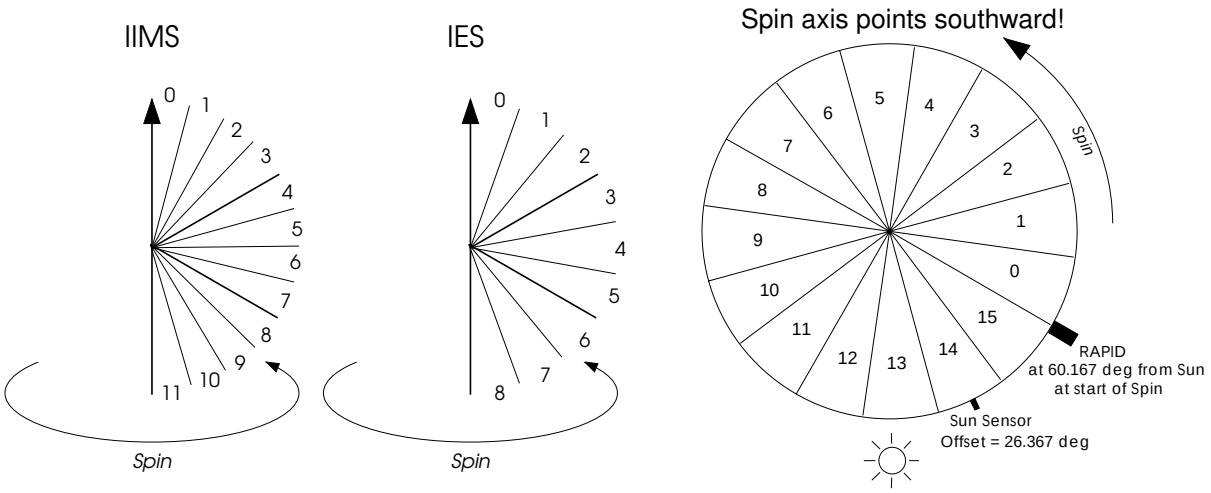

Figure 2: The IIMS and IES polar segments relative to the spin axis (left and center) and the RAPID sectorization relative to the sun (right). *Note that the spin axis actually points towards the −Z GSE axis (southward).*

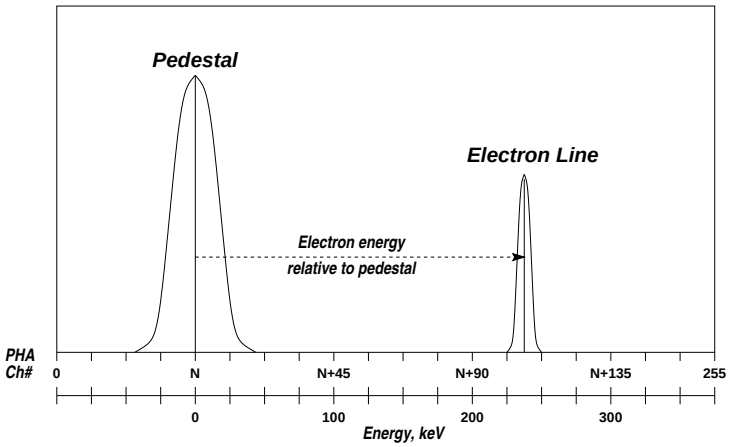

Figure 3: The IES pulse-height analysis. The analog signal, reflecting the electron's energy on top of a background pedestal, is digitized from 0 to 255, and then sorted into broad energy bins that must be set relative to the pedestal.

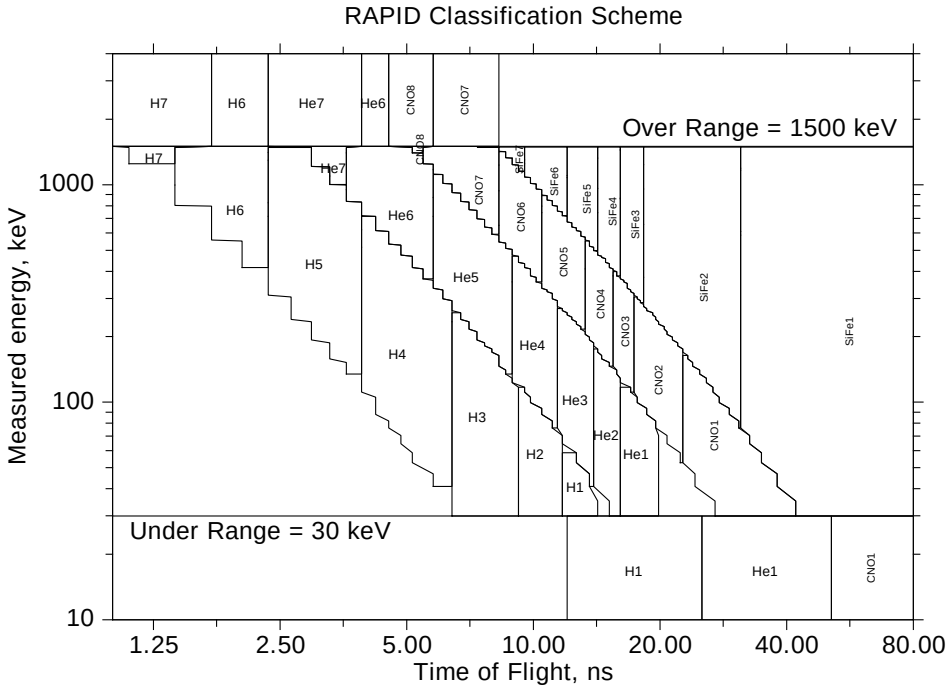

Figure 4: The RAPID ion classification system. Every ion "event" occupies a point in the 256×256 energy-TOF space, which is divided into areas for different ion species and up to 8 energy channels. For events of (internal) energy < 30 keV, no energy signal is produced. In this "underrange" region, species determination is done solely with TOF and the fact that the energy is below this threshold.

The opening angle for a single ion detector is also 60°, but unlike for the electrons, the subdivision into four 15° slots is done by determining the location of the start signal. This of course has an efficiency associated with it.

The start and stop signals are used to measure the time-of-flight (TOF) over the 32 mm separation. This time plus measured energy locate the event within the energy-TOF space of Figure 4 which then determines the species and energy channel. The number of events in each of the species-channel bins in Figure 4 is read out and reset once per sector (1/16 spin).

Only the hydrogen, helium, and carbon-nitrogen-oxygen (CNO) data are delivered by RAPID as part of the regular products; the silicon-iron channels are also available but only in the direct events product (see ICD).

2.3 Spin Sectorization

For both IIMS and IES, the azimuthal distribution of particle fluxes is obtained by sorting the counts into 16 sectors during one rotation of the spacecraft (right side of Figure 2).

The spin phase relationship between the sun sensor pulse and the start of sector 0 (the start of a new spin) is fixed so that the RAPID detectors are looking into the direction of the sun at sector 13.326, or about one third into sector 13. (This relationship has been set in agreement with the other experiments so that all start a new spin simultaneously.)

3 Instrument Operations

3.1 Telemetry modes

The Experimental Data Block (EDB) contains the compressed science data produced by the Digital Processing Unit (DPU). One EDB is generated per spin (∼4 s). The data structure varies with the telemetry mode. The RAPID telemetry formats are:

NM: Nominal mode is active most of the operation time of the instrument with 1024.8 bits/second.

BM: Burst mode allows four times more data downlinked than NM. The principal difference between BM and NM is a higher sampling rate for the 3-D ions and an enhanced 3-D electron products.

BM3: This mode, lasting ∼5 minutes once a day, is intended to read out scratch memories of some instruments. For RAPID, BM3 simply forms a data gap during this time.

NM3: Nominal mode 3 is a special mode on SC2 only, used between July 2003 and April 2004; in this mode, RAPID "borrows" extra bandwidth from the non-functioning CIS instrument so that the data are in BM format even though the spacecraft telemetry mode is NM. The times for NM3 can be found under the following link:

`http://caa.estec.esa.int/caa/rapid_docs.xml`

Note: NM3 was an attempt to improve the angular resolution of the electron 2-D data in NM. It became unnecessary after May 2004 when the new `L3DD` product became available on all 4 spacecraft (see Section 5.1.1, page 14 and Table 2).

The telemetry modes can be checked in the RAPID *Quicklook Plots,* described in Section 5.4 and available at `http://caa.estec.esa.int/caa/quicklook.xml` by selecting plot `C*_CG_RAP_SUMPLOT_D` in the 6th panel — *IIMS Modes, TM*. Alternatively this information is also contained in the CAA *"Status"* product `SETTINGS` (see Section 5.3).

3.2 Operations on IES (electrons)

3.2.1 Integration time

The RAPID detectors do not accumulate counts all the time; there is a *dead time* that leads to a *duty cycle* of less than 100%.

The total energy deposited by electrons during the so-called *integration time* is accumulated and then read out over the next 50 μs (this is so-called dead time which is fixed for all integration times). The integration time switches automatically between values of 2, 5, 15, and 50 μs, depending on count rate. It is vital that at most one electron per interval (integration time) is detected, otherwise it is the summed energy of multiple electrons that is registered. Thus the integration time should be as short as possible. On the other hand, it is desirable to have a long integration time to improve the duty cycle. The maximum duty cycle of 50% is achieved with an integration time of 50 μs. This is the usual case except during times of high count rates.

Caveats:

- There can be jumps in the flux values at such erroneous switching times as the pile-up effects, i.e. more than one count per interval, are suddenly removed. This problem is most serious before January 25, 2002, when the automatic switching was occurring too late. After this date the timing of the auto-switching was improved by modifying the parameters involved. The problem is thus reduced, but not entirely eliminated.

Corrections for this are not possible; the user must be careful with such jumps. An example on switches of the integration time and its effects can be seen in Figure 5.

- From January 18 to February 20, 2004, the automatic switching on SC4 was turned off by error; the integration time remained fixed at 50 μs (Figure 6).

The information on integration time switches can be found in the *Quicklook Plots,* by selecting plot `C*_CG_RAP_SUMPLOT_D`, 5th panel — *Int Time*. This information is also available in the *"Status"* product `SETTINGS` (Section 5.3).

3.2.2 Histogram mode

Histogram mode is a test mode that is commanded about once month. A fixed integration time is selected, histogram mode activated, the counts in all 256 energy channels are read out for all 9 angular detector strips, uncompressed, and then regular operation is resumed.

Times when IES was switched to the histogram mode will be reflected in the *Quicklook Plots,* plot `C*_CG_RAP_SUMPLOT_D`, 5th panel — *AutoSW*.

A complete list of times when histogram mode occurs is given in the table at:

`http://caa.estec.esa.int/caa/rapid_docs.xml`

3.3 Operations on IIMS (ions)

3.3.1 IIMS instrument modes

In the usual *serial* mode, each ion head accumulates for a fixed 60 ms within each of the 16 azimuthal sectors, one after the other. This means the duty cycle depends on spin rate. For example, for a nominal 4 s spin, each of the 16 sectors requires 250 ms, so each head accumulates for only 24% of the time. During the remaining dead time, the counts from the previous sector are processed and other housekeeping tasks are performed.

There is also a *parallel* mode that was used occasionally in the solar wind early in the mission; in this mode, all three heads accumulate simultaneously for 180 ms per sector.

In the first few months of the mission, before the main patch was uploaded, the accumulation times were 65 and 195 ms for serial and parallel mode, respectively.

The IIMS instrument modes can be checked on then *Quicklook Plots*, plot `C*_CG_RAP_SUMPLOT_D` in the 6th panel — *IIMS Modes, A*. This information is also available in the *"Status"* product `SETTINGS` (Section 5.3).

3.3.2 Damage of the central ion head

- The central ion head on all 4 spacecraft deteriorated within the first months of the mission; most likely sunlight saturated the time-of-flight system. The result is that ion distributions are not available within 30° of the ecliptic plane. This is often referred to as the "donut" effect (hole in the middle). How this caveat affects the 3-D distribution see Figure 7. For the omni-directional flux products the "donut" effect is taken into account.

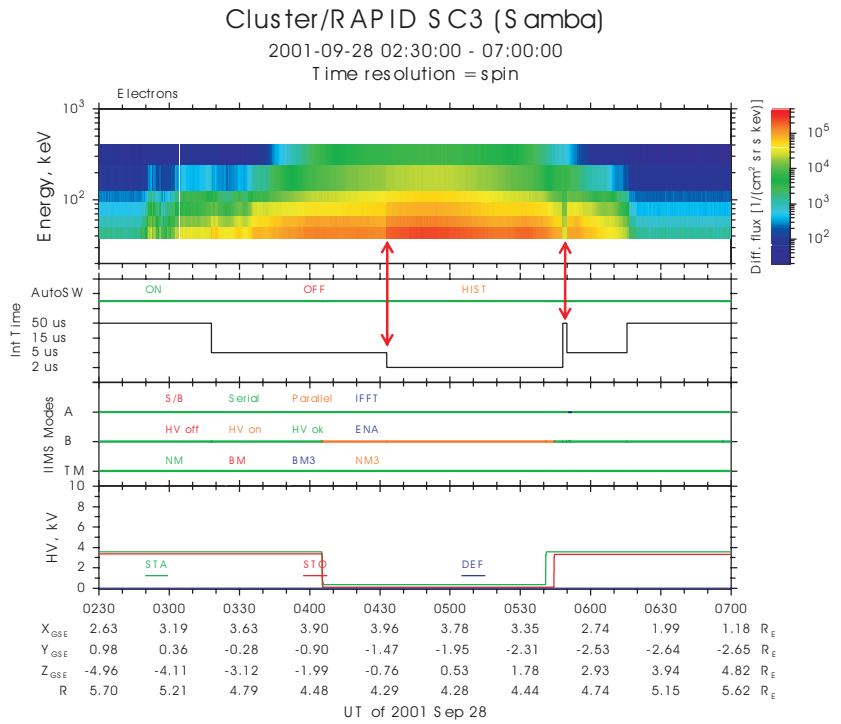

Figure 5: Demonstration of how changes in the IES integration times can produce erroneous changes in the electron fluxes if the automatic switching occurs too late (times are denoted by red arrows). For example at ∼04:32 integration time (second from the top panel) switches from 5 μs to 2 μs and produces the sudden sharp change in the electron intensity. Another example one can see at ∼05:49, when integration time was erroneously switched from 2 μs to 50 μs and than back to 5 μs producing a sharp intensity drop for the time of the too long integration time.

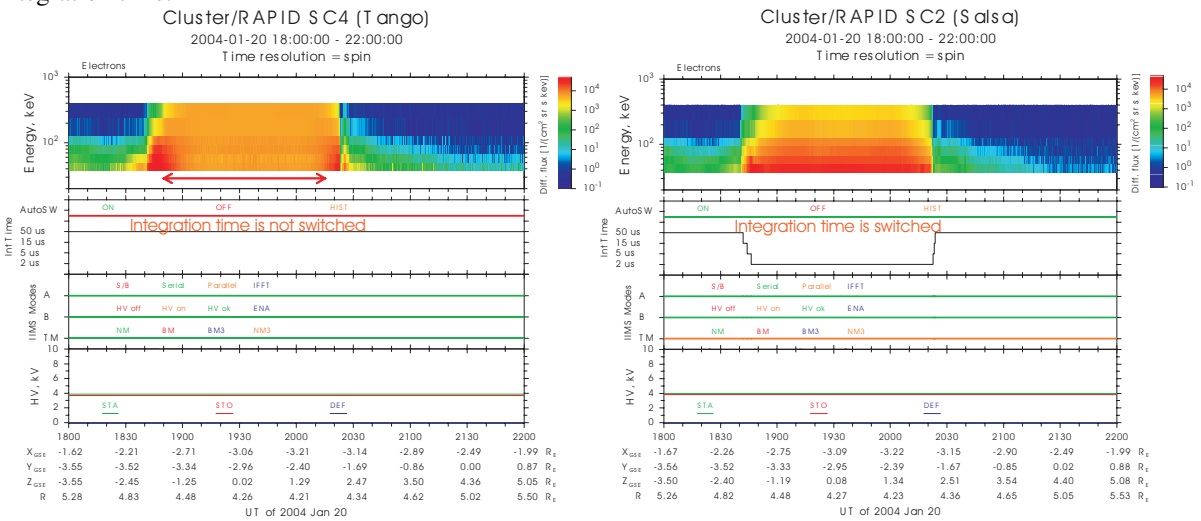
Cluster/RAPID SC4 (Tango)
2004-01-20 18:00:00 - 22:00:00
Time resolution = spin
Integration time is not switched
Cluster/RAPID SC2 (Salsa)
2004-01-20 18:00:00 - 22:00:00
Time resolution = spin
Integration time is switched
UT of 2004 Jan 20

Figure 6: Left: An illustration of what can happen when the integration time fails to switch. As the intensities increase, the count rates in the lowest channels are too low, since multiple low-energy events count as a single high-energy one. Right: For a comparison the same time period and the same region measured by another Cluster spacecraft where the auto-switching was working properly.

3.3.3 Loss of Ions on SC1 since March 16, 2007

- On March 16, 2007, the MCPs on SC1 started behaving strangely, with loss of time-of-flight signals. Some weeks later, the voltages became unstable, so they were shut down. As a result, there are no ion data from SC1 since this date.

4 Measurement Calibration and Processing procedures

Before raw data become scientifically valuable they need to go through various treatment procedures and become reprocessed. Imperfection of some corrections lead to caveats which the user should be aware of.

4.1 Electrons

- **Spectra correction**

  Since the pedestal position (see Section 2.1) moves with time (aging), temperature, and even raw count rate, its position is constantly monitored and corrected for in the data. A consequence of this is that the different electron detector strips effectively measure different energies. Efforts are made to correct for this, as described in Section 4.3. However, the corrections are not always perfect and the user should be aware of this. For diagnostics when pedestal is an issue see RAP-CR.

- **Pedestal noise correction on SC4**

  Pedestal contamination affects the electron omni-directional distribution. To correct for this, we remove the noisy strips from both the omni-directional and 3-D data. Correction, as always, is made for the fluxes only, never for the raw count rates. For more details and examples see RAP-CR.

- **Solar noise correction on SC3**

  Sunlight enters the IES head 1 on SC3 and produces noise in the data. This solar noise is very strongly dependent on solar aspect angle (SAA). A correction is made to both 3-D and omni-directional flux data. For more details about this correction and examples see RAP-CR.

- **Inter-spacecraft cross-calibrations**

  Large differences between the electron detectors on different spacecraft are not expected and spot checks have confirmed this expectation.

4.2 Ions

- **Time-varying detector efficiencies**

  The start and stop signals are generated by MCPs, whose performances change considerably over time. Thus the overall response, including the TOF efficiency, is monitored continuously and the calibration files regularly updated. The user must realize that since these parameters are based on long-term averages (over weeks or months) there can be deviations on any particular day. See more details and diagnostics in RAP-CR.

- **Absolute fluxes may be overestimated**

  As illustrated in RAP-CR (Section 6.1), comparisons with the CIS/CODIF instrument indicate that at times when the TOF efficiencies are fairly low the derived geometry factors might be underestimated, hence producing fluxes that are too large.

- **Inter-spacecraft and inter-head cross-calibrations**

  Efforts are made to cross-calibrate the ion detector performances over the 4 spacecraft and all the functioning heads, by normalizing them such that on the long term they all have the same average values, see RAP-CR. The user must realize that these inter-spacecraft/inter-head cross-calibrations are therefore only approximate and can deviate on any particular day. This could lead for example to an assymetry between ion head 1 and 3.

- **First energy channel (He, CNO)**

  These channels are included in raw count rates but they are replaced with fill values in particle flux datasets. The lower part of Figure 4 shows the "underrange" region, where no energy signal is received (<30 keV); ion classification is done solely on TOF information and the fact that the energy is so low. These events contribute to energy channel 1. The species determination is not so precise: low energy hydrogen enters and dominates the helium channel 1 (which is therefore suppressed) and the CNO channel 1 often exhibit signs of contamination as well, most likely from low energy helium. For more detail, see RAP-CR.

- **Accumulation problem for the 3-D ions, SC1, 3, 4, NM**

  There is a bug in the onboard programming that causes the 3-D ions to be accumulated at different times in different sectors. A presentation of this bug is shown in Figure 7. Therefore, the users dealing with the ion 3-D distributions (standard), i.e. the merged full ion 3-D data (see Figure 7) should be aware that it could have spurious anisotropy due to different accumulation times. In suspicious cases it is advised to check this, using the ion 3-D distribution (expanded) (see Figure 7) which will show the partial distributions in a time sequence as they were accumulated.

  This bug affects only the ion data in nominal mode, and only spacecraft 1, 3, 4.

4.3 Standardized Energy Channels

A uniform set of energy channel definitions is essential for any physical analysis of the data. Hence, the variations in the spectra among the sensors are corrected to bring them effectively to such a standardized set. The correction is applied to the each ion and electron sector. The "official" values now used for the CAA products are listed in Table 1.

The algorithm used for this correction is to fit the data between adjacent channels to a power law which is then integrated over the energy shift region, with the resulting flux subtracted from the one and added to the other channel, as shown in Figure 8.

For the electrons, there is a further adjustment to be made: because the pedestal that defines the energy origin can move in a way that depends on count rate, its location is monitored by some additional diagnostic channels. The spectral shift introduced by this effect can be deduced and then also corrected for as part of the energy channel standardization.

Note that the spectral correction is applied only to flux data, not to the raw count rates since they are to remain as original raw data.

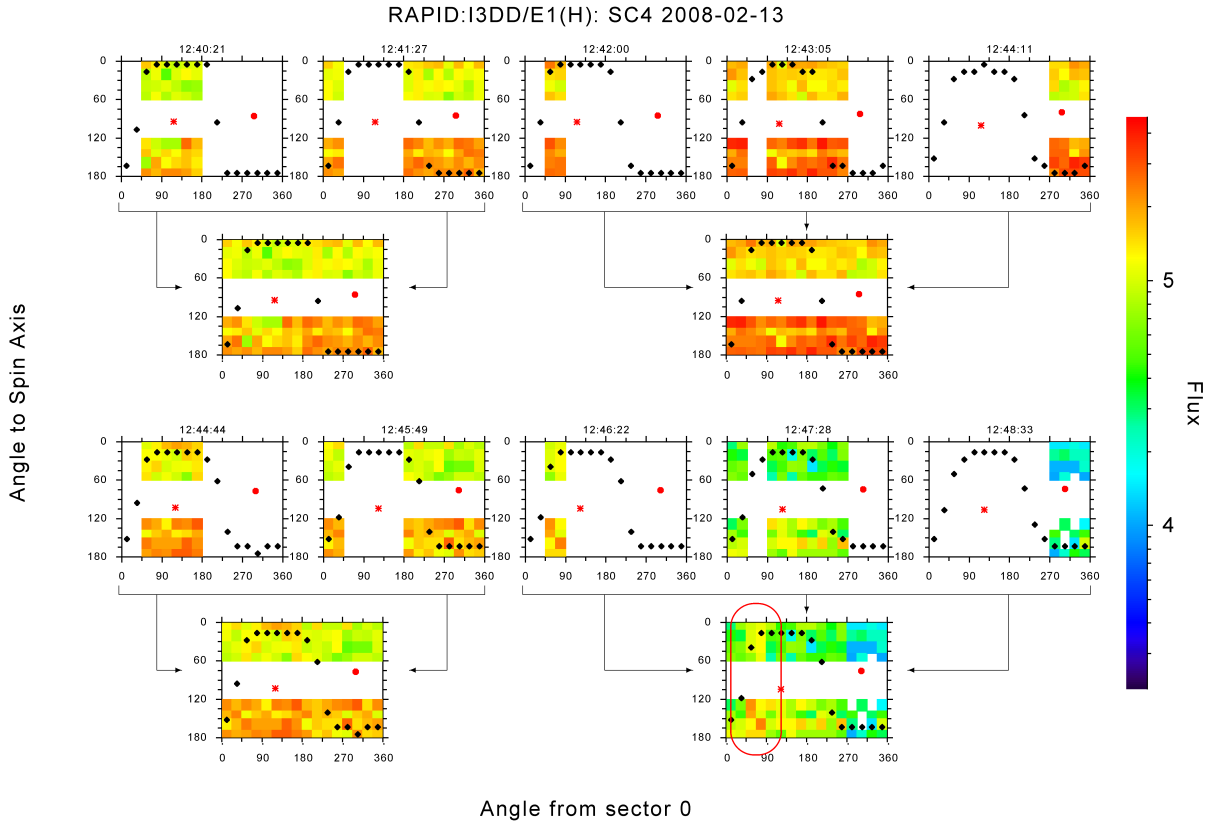

Figure 7: Example of the 3-D ion timing problem. Rows 1 and 3 show the partial distributions, the dataset called as the ion 3-D distribution (expanded) at the CAA, while rows 2 and 4 are the merged full distributions (the ion 3-D distributions (standard) at the CAA). The red oval at the lower right indicates a spurious anisotropy that is really time-aliasing.

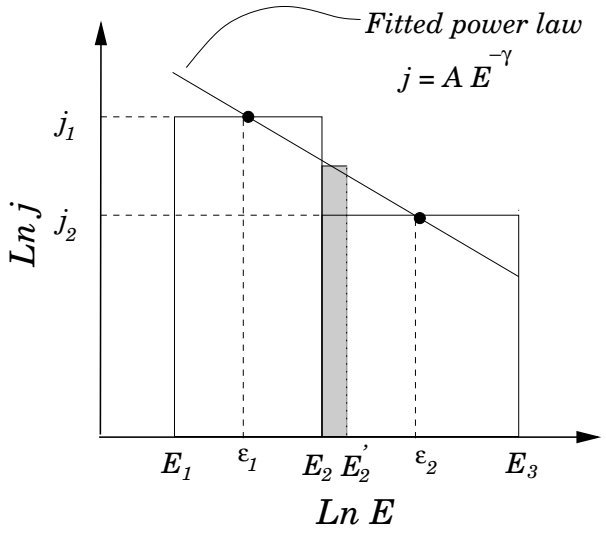

Figure 8: Shifting the energy threshold between two channels: the differential flux in two channels is fitted to a power law, that fit is integrated over the energy shift $E_2' - E_2$ (shaded area), and the result moved from one channel to the other.

4.4 Phase Space Density Conversion

Conversion factors between differential flux and phase space density are listed in Appendix C.

5 Key Science Measurements and Datasets

5.1 Particle Distribution

Key science measurement for the RAPID instrument are particle distributions in the following units:

Raw Count Rate These are raw data in units of (1/s) with no corrections, calibrations, suppressions whatsoever; only the *accumulation time* is employed to convert from counts to rates. This accumulation time is well-defined but not trivial to determine, hence it is included as a record-varying parameter in every count-rate dataset. The original number of counts can thus be reconstructed if wanted. The dataset names of the raw data products have an ending suffix _R (see Appendix A for a complete list of datasets).

Number Flux Processed data in units of *differential particle flux*, 1/(cm^2 sr s keV). See ICD for more details.

Standard Deviation For both fluxes and raw count rates, the *standard deviation* is also included in each record, in the same format and array size as the data. This is obtained from both the Poisson statistical error of the counts plus a factor for the data compression uncertainty; the former normally dominates.

For measured zero flux, the standard deviation is also set to zero, although it should really be that for a single count, to express the uncertainty level. However, such a procedure would lead to errors when summing over longer times. Recall that errors are combined by summing the variance, i.e. the sum of the squares of the standard deviations.

Time Tag The record time tag refers to the middle of the record interval; the time-half-interval for each record is also given.

Note that the record interval and the accumulation time are two separate things: data are accumulated over a certain interval but not necessary for 100% of that time.

5.1.1 Electrons

The electron distributions as delivered directly by IES exhibit some importance differences between the nominal telemetry mode (NM, low bit rate) and burst mode (BM, high bit rate), see Section 3.1. All the above products have a time resolution of one spin, i.e. ~4 s.

Here we list only the datasets in particle flux. The datasets in raw count rates have an additional suffix _R in their names as indicated by the * in the names below. They can be downloaded as well but their use is advised only for experts as these datasets are not calibrated and corrected.

Omnidirectional: Omnidirectional electron fluxes are created artificially for CAA from the 3-D/2-D data by summing up over the polar and azimuthal angles. It always has the 6 energy channels of nominal mode: array size {6}.

- Dataset title: Electron, omni-directional distribution (dataset id `ESPCT6*`)

Electrons Lite: Since May 2004, a new 3-D electron product is available in nominal mode. It is the same as the burst mode distribution but for energy channels 1 and 3 only. For CAA, this product is also provided in burst mode, by simply extracting it from the existing burst mode distribution. The array size is {2,16,9} for energy, azimuthal direction, polar direction.

- Dataset title: Electron, 3-D distribution (standard) (`L3DD*`)

Burst mode: There is one full 3-D electron distribution per spin, with 9 polar directions, 16 azimuthal sectors, and 8 energy channels.

The polar directions 0–2 and 6–8 (those closest to the spin axis, Figure 2) really have only 8 azimuthal sectors per spin; the CAA products artificially double this to simplify handling the data as a rectangular array of size {8,16,9}.

- Dataset title: Electron, 3-D distribution (`E3DD*`)

Nominal mode: Counts are summed over the whole spin, so angular information is limited to 9 polar directions; thus this is often called 2-D data, as reflected in the CAA product name. There are also only 6 energy channels, the top two corresponding to the upper 4 in burst mode. The array size is {6,9}.

- Dataset title: Electron distribution (spin-averaged detector) (`E2DD6*`)

Sparse 3-D: This product exists only until May 2004 (the CAA data files are empty after this), when it was replaced by Electrons Lite (see above).

To compensate for the missing 3-D data in NM, this additional product, called EPAD (*electron pitch angle distribution*) contains fluxes from 3 polar directions for azimuthal 16 sectors, but only for two energy channels. One direction is perpendicular to the magnetic field in that sector, the 2nd is 90° to the first, the 3rd is either parallel or anti-parallel to the spin axis. The other 6 directions are given as fill values. An example of the angle-angle plot created with this product see in Figure 9.

The definitions of the two energy channels have changed several times over the first years of operation;

Table 2: A summary table of characteristics for different datasets

Species	Dataset title	Dataset name	Nominal mode	Burst mode
Electrons	Electron, omni-directional distribution	`ESPCT6`	6 energy channels	6 energy channels
	Electron, 3-D distribution (standard)[a]	`L3DD`	9 polar × 16 azimuthal 2 energy channels	9 polar × 16 azimuthal 2 energy channels
	Electron, 3-D distribution (best)	`E3DD`		9 polar × 16 azimuthal 8 energy channels
	Electron distribution (spin-averaged detector)	`E2DD6`	9 polar × 1 azimuthal 6 energy channels	
	Electron 3-D distribution (sparse)	`EPADEXm`[b]	3 polar[c] × 1 azimuthal 2 energy channels	9 polar × 1 azimuthal 2 energy channels
Ions	Ion, omni-directional distribution	`HSPCT`, `ISPCT_He`, `ISPCT_CNO`	8 energy channels	8 energy channels
	Ion, 3-D distribution (standard)	`I3DM_H`, `I3DM_He`, `I3DM_CNO`	12 polar × 16 azimuthal 8 energy channels	12 polar × 16 azimuthal 8 energy channels
	Proton 3-D distribution (sparse)	`IPADEX`[d]	3 polar[c] × 1 azimuthal 2 energy channels	3 polar[c] × 1 azimuthal 2 energy channels
	Ion, 3-D distribution (expanded)[e]	`I3D_H, I3D_He, I3D_CNO`	12 polar × 16 azimuthal 8 energy channels	12 polar × 16 azimuthal 8 energy channels

[a] The product is available since May 2004.
[b] The product ceases after May 2004.
[c] Particles are registered in only 3 of 9 directions, as determined by onboard magnetic field measurements.
[d] After May 2004 this product is available only in burst mode.
[e] Expanded 3-D distributions are split into partial distributions according to different accumulation intervals.

hence 3 separate products must be given, distinguished by m=1, 2, 3:

m	From	To
1	—	May 2001
2	May 2001	July 2002
3	July 2002	April 2004

The above dates are approximate, and vary slightly for each spacecraft. The data files are empty for the times for they do not apply. No energy corrections are applied for this product.

Strictly speaking this product exists only in NM, in BM it is emulated from BM and it contains 9 polar directions.

- Dataset title: Electron 3-D distribution (sparse) (`EPADEX`m`*`)

All the above products have a time resolution of one spin ≈4 s.

5.1.2 Ions

The ion distribution products delivered directly by IIMS can be summarized as follows.

Omnidirectional: There is an omni-directional base product for H, with 8 energy channels. Since these events do not depend upon the efficiency of the directional signal mentioned above, they are not identical to the sum of the 3-D data. Array size is {8}, frequency is once per spin.

There are also omni-directional He and CNO spectra at a rate of one per 4 spins: their array sizes are {8}.

- Dataset titles: Proton (Helium, CNO), omni-directional distribution (`HSPCT*, ISPCT_He*, ISPCT_CNO*`)

3-D Data: *The merged full distributions of ion fluxes* for 3 species (H, He, CNO) in 12 polar and 16 azimuthal directions over 8 energy channels. Array size is {8,16,12}.

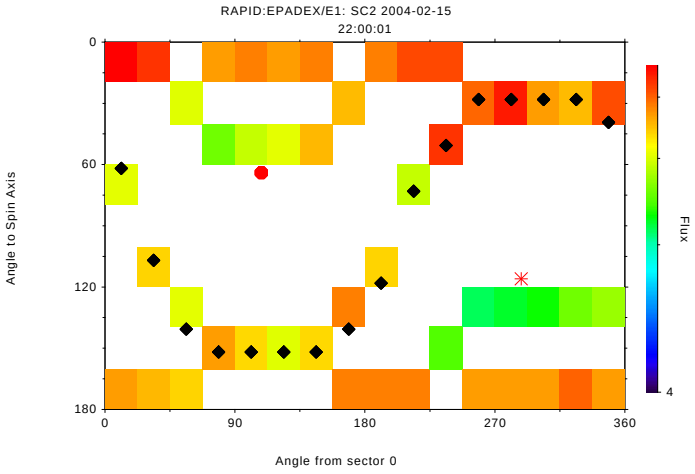

Figure 9: An example of the sparse 3-D electron distribution in s/c coordinates. Black diamonds indicate 90° to the magnetic field, and the red dot and red star mark the calculated direction magnetic field vector (taken from FGM). Therefore, the data obtained in the direction perpendicular to the magnetic field are seen along the black diamonds, the data in second direction, perpendicular to the first, are seen around the red dot and star and eventually the data accumulated in the parallel or anti-parallel to the spin axis direction are seen in the polar sectors 0 (0–20°) and 8 (160–180°).

Each distribution is accumulated over 8 spins, except on spacecraft 2 where they are accumulated over a single spin. Because of the limited telemetry rate for RAPID, only a fraction of accumulated data can be transmitted to the ground. In burst mode, one can transmit one full distribution over 8 spins, whereas in nominal mode, it requires 32 spins. This is a result of the limited telemetry rate for RAPID. There are thus data gaps between the delivered accumulations.

Note that the proper distributions are the partial ones described next. The merged ones are reconstructed from them for the convenience of the users, but may exhibit time-aliasing problems, as shown in Figure 7. The merged distributions are only provided as fluxes, not as count rates.

- Dataset titles: Proton (Helium, CNO), 3-D distribution (standard) (`I3DM_H, I3DM_He, I3DM_CNO`)

The partial distributions of ion fluxes for 3 species (H, He, CNO) in 12 polar and 16 azimuthal directions over 8 energy channels. Array size is {8,16,12}.

As mentioned in Section 4.2 the I3D distributions for SC1, 3, 4 in NM have a bug in accumulation time and therefore for each time tag corresponding 3-D distribution is not full. In order to indicate how the partial distributions are to be merged to regenerate the full distribution, a *record key* variable named `Rec_Key` is provided for each record. This is an integer with the following values:

Value	Meaning	Sectors included
11	Rec 1 of 1	0–15 (all)
21	Rec 1 of 2	2–7
22	Rec 2 of 2	0, 1, 8–15
31	Rec 1 of 3	2, 3
32	Rec 2 of 3	0, 1, 4–11
33	Rec 3 of 3	12–15

Note that the value 11 is provided for burst mode and SC2 for which no splitting is done: each record is a complete simultaneous distribution.

- Dataset title: Proton (Helium, CNO), 3-D distribution (expanded) (`I3D_H*, I3D_He*, I3D_CNO*`)

Sparse 3-D: As for the electrons, there is a sparse 3-D hydrogen distribution available every spin, with 3 polar directions per sectors, which vary with the magnetic field. It too is expanded to fill the complete 3-D array with fill values for those directions not measured. The array size is {2,16,12}.

As of May 2004, this product exists only in burst mode.

- Dataset title: Proton 3-D distribution (sparse) (`IPADEX*`)

5.1.3 Pitch Angle Distributions

The pitch angles for electrons and ions are delivered based on the 5-vectors-per-second (5VPS) FGM data. Each distribution is accompanied by the GSE components of the magnetic field averaged over the data interval plus a quality flag. This flag is derived from the normalized variance of the field such that it is 1 for steady (constant) field and 0 for extremely variable.

Electrons: Differential fluxes in 9 pitch angle bins (0–180°) are available in burst mode, 8 energy channels and after May 2004 in nominal mode, 2 non-contiguous energy channels. The distribution is provided once per spin.

- Dataset title: Electron Pitch Angle distribution (standard, best) (`PAD_L3DD, PAD_E3DD`)

Ions: Differential fluxes in 9 pitch angle bins (0-180°) and 8 energy channels.

Ion pitch angle distributions are provided for
SC2: over 1 spin every 32/8 spins (NM/BM)
SC1, SC3, SC4, BM: over 8 spins once every 8 spins
SC1, SC3, SC4, NM: 8 spins with asynchronous sectors over 24 or 40 spins (a result of the bug illustrated in Figure 7)

- Dataset title: Proton (Helium, CNO) Pitch Angle distribution (standard) (`PAD_H, PAD_He, PAD_CNO`)

5.2 Auxiliary

Some additional datasets are provided to assist users with the interpretations; their derivation requires detailed knowledge of the RAPID location on the spacecraft, the spin axis, and sun sensor. Thus all this is worked out for the user, as separate products.

Flow directions: For each of RAPID's 9×16 (electrons) and 12×16 (ions) polar-azimuth directions, the GSE coordinates of the *flow* vector at their centers are provided. Since these values change very slowly, they are only given once per hour.

- Dataset title: Electron (Ion) Flow direction matrix, RAPID to GSE rotation (`EFLOW_GSE, IFLOW_GSE`)

SC-GSE rotation matrix: Provided in the same files as the flow directions is the actual 3×3 rotation matrix to do a general transformation to GSE from the RAPID spacecraft frame (θ = angle to spin axis, ϕ = sector $\times 22.5°$). See Appendix D for usage.

- Dataset title: Electron (Ion) Flow direction matrix, RAPID to GSE rotation (`EFLOW_GSE, IFLOW_GSE`)

Pitch Angles: For each of the electron and ion polar-azimuth flow directions, the angle to the magnetic field (pitch angle) plus a magnetic azimuth is provided; this is done for each spin.

- Dataset title: Electron (Ion) pitch angle assignment matrix (`EPITCH, IPITCH`)

What is necessary in order to plot 3-D angle-angle plot

- One can create angle-angle plots from 3-D distributions (in any units): `E3DD`, `L3DD`, `I3DM_H`, `I3DM_He`, `I3DM_CNO`, `I3D_H`, `I3D_He`, `I3D_CNO`, `EPADEXm`, `IPADEXm`
- `EFLOW_GSE or IFLOW_GSE`: the rotation matrix for rotation from SC to GSE coordinates
- Spin resolution or 5VPS FGM magnetic field vector: in the case the magnetic field direction will be plotted (see white and red dots in Figure 10).

5.3 Status

The key two datasets for knowing the instrument status are CAVEATS and SETTINGS.

The `CAVEATS` dataset text contains warnings or information on data gaps. Some of these are generated automatically by the processing software, while others are copied from a master list maintained by the RAPID Team. The daily caveat files contain only those caveats that are relevant to that one day.

Each caveat text has an associated *time range* which is always truncated to fit within the time limits of the given file. This means it does not represent the true overall time limitation of the text. In such cases, the text itself specifies when the warning starts and stops.

The `SETTINGS` dataset contains a subset of the housekeeping data, 11 variables in all, for the most important aspects of the instrument status including telemetry mode, multichannel plate voltages, electron integration time, ion accumulation mode. These variables are described in RAP-ICD as well as by the dataset metadata.

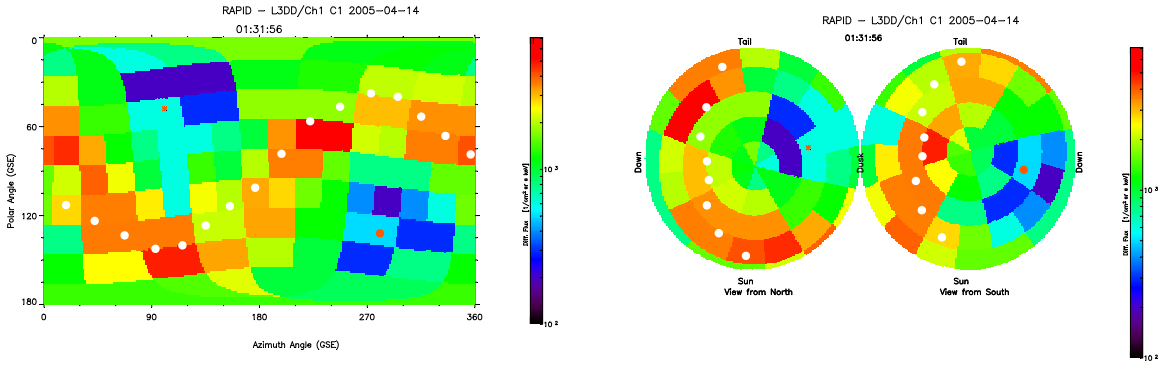

Figure 10: Left: 3-D electron distribution from L3DD data in GSE showing 9 polar directions and 16 azimuthal sectors. Right: The same data but in a bispherical view, whereas the left spheres on both plots show northward flow and the right southward. White dots indicate 90° to the magnetic field, and the red dot and red star mark the calculated direction magnetic field vector.

5.4 Graphical

RAPID summary plots are available for differential fluxes. In Figure 11 we present an example plot of Cluster 1. From top to the bottom omni-directional differential energy flux spectra of electrons, hydrogen, helium, and CNO with 1-min time resolution for January 25, 2005 within a 6 hour period from 12:00 to 18:00 UT are shown. At the right hand side of each plot panel a colour bar defines the colour code of the spectra. This range is autoscaled, which has to be considered when comparing several plots.

The second part of the plot (panels 5-7) reflects the IES and IIMS instrument settings. For more information about instrument settings and their meaning see the description in Section 3 and RAP-ICD.

At the bottom of the summary plots orbit information in GSE coordinates is given.

The Summary Plots can be downloaded from CAA as part of the RAPID *ancillary* data or viewed under the CAA Quicklook plots. They may also be obtained from the MPS web site at `http://www.mps.mpg.de/cgi/rapid/sumplot.cgi`.

5.5 Dataset Version

Currently RAPID data at CAA are of the 2nd release, with upgraded calibrations over those of the 1st release.

The calibration version can be found in the data files. There is a metadata parameter called `DATASET_VERSION`, which for RAPID is a 4-digit code, which is slightly different for electrons and ions.

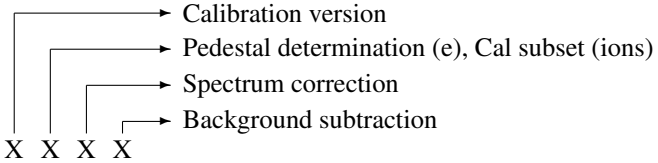

Calibration version has the value of 2 or 3 (see caveat below) for the current calibration data; or 1 for the old calibrations of the 1st release (now obsolete).

Pedestal determination for electrons; how the pedestal (Figure 3) is determined: 0 for no correction, 1 for the "stepping" method, the only method used at the moment.

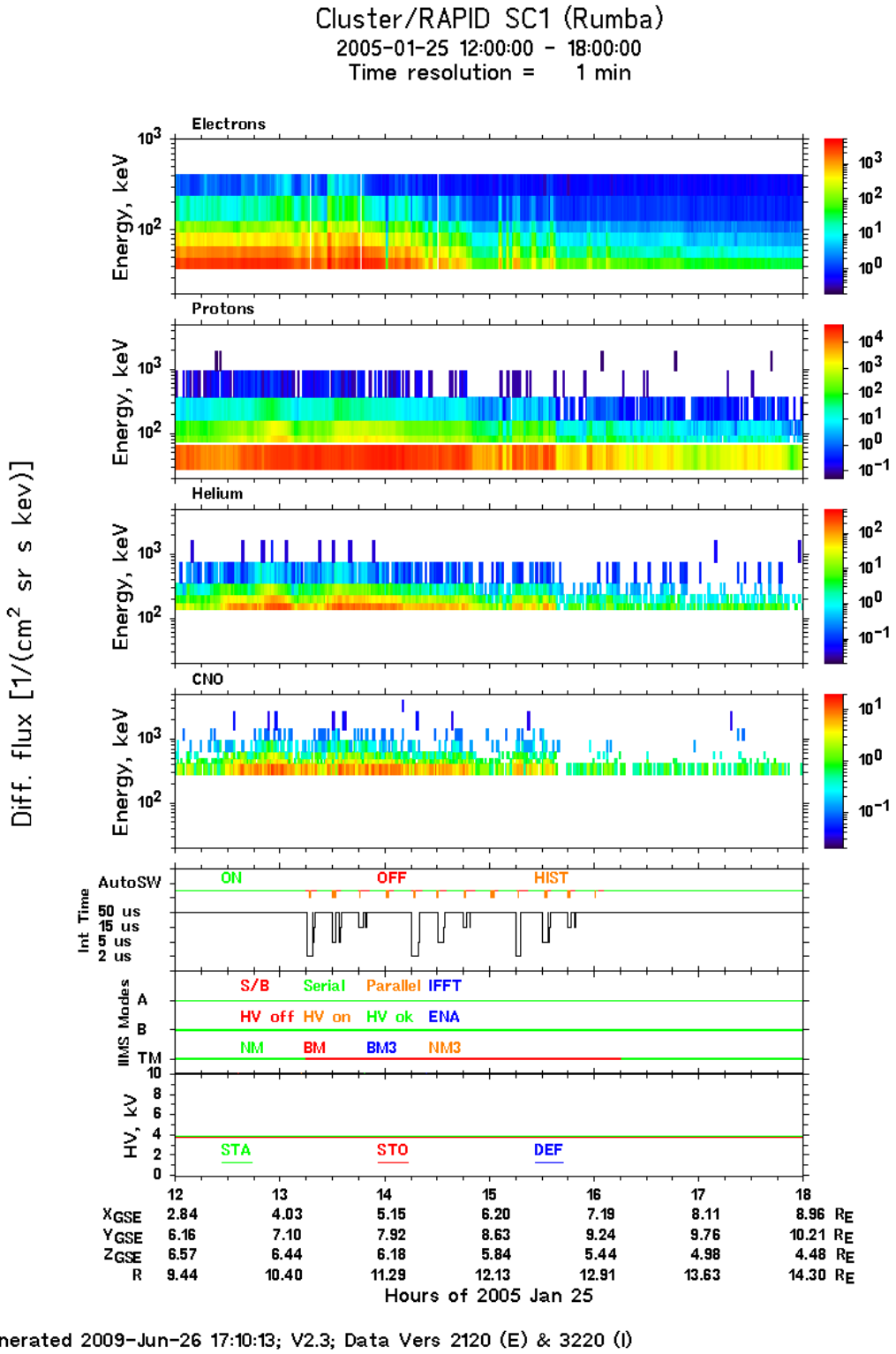

Figure 11: Example of a CAA RAPID summary plot. Panels 1–4 show from top to bottom differential fluxes of ESPCT, HSPCT, ISPCT_He, and ISPCT_CNO. Panels 5–7 display several instrument settings.

Cal subset for ions; for internal RAPID usage: the data at CAA always have the value 2.

Spectrum correction how the varying energy thresholds between detectors, spacecraft, and (for electrons) integration times are corrected to a uniform set of values. The pedestal shift for electrons is also corrected with spectral shifting. Possible values are: 0 for no correction, 2 and 3 for power law fitting between two adjacent channels. With 2, the pedestal shift is the spin average, while for 3, it is done for each sector. So far only 2 is used.

Background subtraction 0 for no subtraction; 3 for removal of solar noise on SC3 (Section 4.1).

Caveat:

- In January 2009, an error was discovered in the ion geometry factors for 2006 and later. As a result, the 2006 *ion flux products* (`HSPCT`, `ISPCT_He`, `ISPCT_CNO`, `I3D_H`, `I3D_He`, `I3D_CNO`) have been redelivered to CAA. To distinguish the corrected datasets from the previous ones, the dataset version number for ions now begins with 3. For other products and for ion data from 2005 and earlier, the initial digit remains 2 (for now).

5.6 Quality flag

Every CAA RAPID data product contains the quality flag. In fact, this is the calibration version for a given calibration set (constant number). The user should see the caveat files for detailed issues.

6 Recommendations

Most straightforward to use are the omni-directional particle fluxes for ions and electrons.

A summary of the RAPID Datasets at the CAA is listed in Appendix A.

A guide on calculations of the RAPID partial moments can be found in Appendix B.

Conversion factors between differential flux and phase space density are listed in Appendix C.

6.1 Usability issues

Regions where the instrument operates well: These are plasma sheet, magnetosheath, magnetopause, cusp, bow shock, upstream region, in cases where for ions the main plasma flow direction does not coincide with the look direction of the dead sensor.

Regions where there are issues: The radiation belts is a region where a user must be careful with the data analysis. In this region the pileup problems can lead to the flat spectrum, see Section 3.2.1 and Figure 6. Also here often appear problems with the auto-switching of the integration time and as a sequence erroneous jumps in the fluxes, see the same section and Figure 5.

Additionally at ~3-5 L-shells more energetic ions and electrons can penetrate the IES instrument, see Figure 12.

The IIMS instrument is not so sensitive to the penetrating particles because of time-of-flight filtering. The pileup effects, from both penetrating particles and high count rates can be detected and will be flagged in future.

Solar Proton Events: can also produce penetrating radiation that distorts the instrument's behavior, see an example in Figure 13.

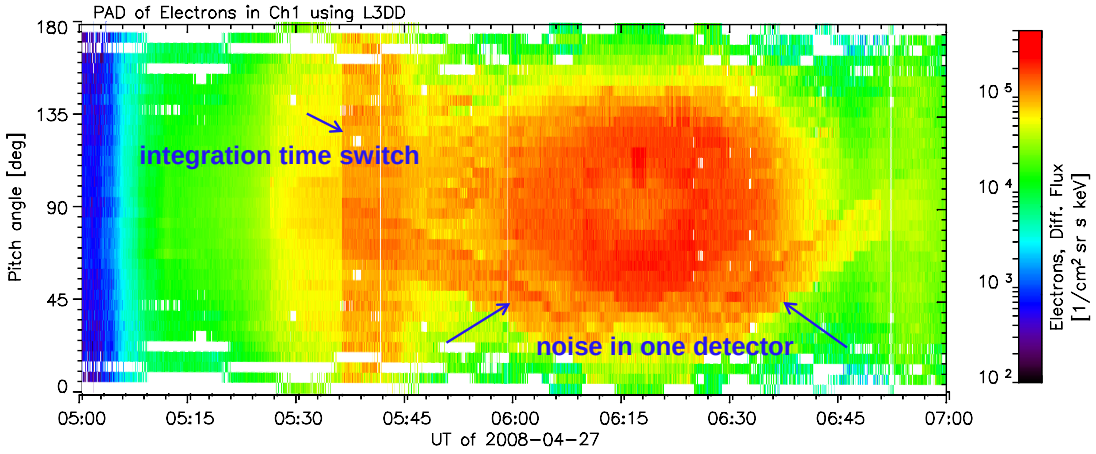

Figure 12: An example of the electron data contamination in the radiation belts. In the pitch-angle distribution of the electrons one could see stripes denoted as the noise in one detector. The fact that this noise appears only in the radiation belts implies that the contamination is from penetrating particles. The sharp enhancement of the electron flux at the integration time switch is not related to the contamination problem.

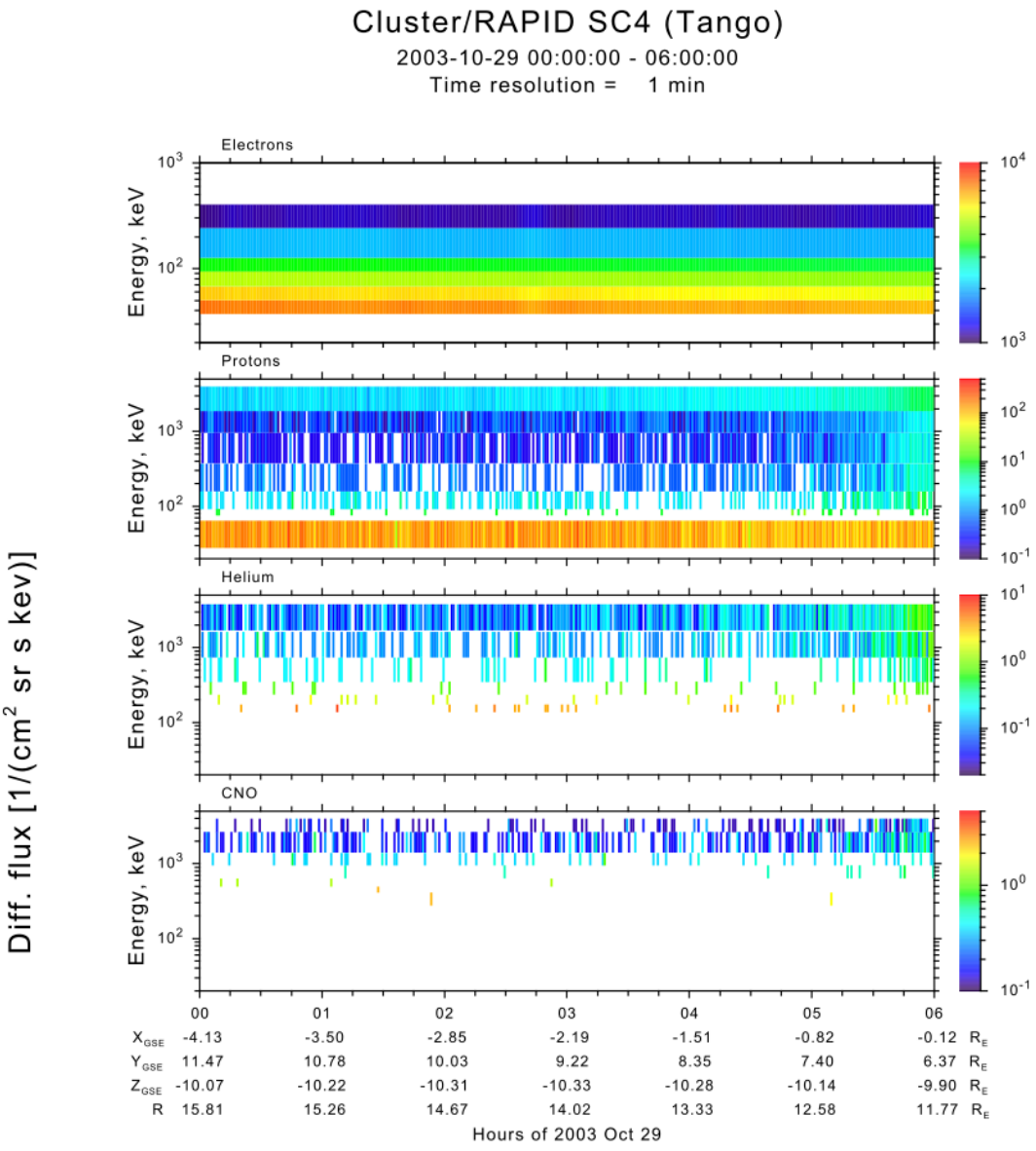

Figure 13: An example of the effects which produce penetrating particles during the Halloween solar proton event. Electrons do not show sensible measurements. Ion intensities increase with the energy, when they expected to decrease towards the higher energy channels.

Appendices

A Summary of RAPID Datasets at CAA

Note: the dataset IDs marked with * are available both as differential fluxes and as counts/sec (with suffix _R).

Table 3: A summary table of RAPID datasets (in dataset id, * is for _R in raw count units).

Dataset title	Dataset ID
Science	
Particle Distribution	
Electron, omni-directional distribution	ESPCT6*
Electron, 3-D distribution (standard)	L3DD6*
Electron, 3-D distribution (best)	E3DD*
Proton, omni-directional distribution	HSPCT*
Proton, 3-D distribution (standard)	I3DM_H
Helium, omni-directional distribution	ISPCT_He*
Helium, 3-D distribution (standard)	I3DM_He
CNO, omni-directional distribution	ISPCT_CNO*
CNO, 3-D distribution (standard)	I3DM_CNO
Pitch Angle	
Electron Pitch Angle distribution (standard)	PAD_L3DD
Electron Pitch Angle distribution (best)	PAD_E3DD
Proton Pitch Angle distribution (standard)	PAD_H
Helium Pitch Angle distribution (standard)	PAD_He
CNO Pitch Angle distribution (standard)	PAD_CNO
Ancillary	
Caveats	CAVEATS
Instrument settings	SETTINGS
Summary Plot	SUMPLOT_D
Electron Flow direction matrix, RAPID to GSE rotation	EFLOW_GSE
Ion Flow direction matrix, RAPID to GSE rotation	IFLOW_GSE
Electron pitch angle assignment matrix	EPITCH
Ion pitch angle assignment matrix	IPITCH
Particle Distribution	
Electron distribution (spin-averaged detector)	E2DD6*
Electron 3-D distribution (sparse): 2001/Feb – 2001/May	EPADEX1*
Electron 3-D distribution (sparse): 2001/May - 2002/Jul	EPADEX2*
Electron 3-D distribution (sparse): 2002/Jul - 2004/Apr	EPADEX3*
Proton 3-D distribution (sparse)	IPADEX*
Helium, 3-D distribution (expanded)	I3D_He*
CNO, 3-D distribution (expanded)	I3D_CNO*

continued ...

Table 3: RAPID datasets, *continued*

Dataset title	Dataset ID
Diagnostics	
Direct Events	DE
Ion diagnostics, SGL1, count rates, nominal mode	SGL1
Ion diagnostics, SGL1, count rates, burst mode	SGL1_BM
Ion diagnostics, SGL2, count rates	SGL2
Ion diagnostics, SGL3, count rates	SGL3
IES pedestal counts in nominal mode	PED_NM
IES pedestal counts in burst mode	PED_BM
IES pedestal positions in nominal mode	PEDPOS_NM
IES pedestal positions in burst mode	PEDPOS_BM
IES Histogram data	HIST
Miscellaneous	
Housekeeping data	HK
Preliminary Energetic Electron, Proton, and Ion Flux, spin resolution	C(n)_PP_RAP
Preliminary Energetic Electron, Proton, and Ion Flux, I minute resolution	C(n)_SP_RAP

B Partial moments

The moments of the velocity distribution function, $f(\mathbf{v})$, of a given particle species are calculated as

$$M_n = \int f(\mathbf{v})\mathbf{v}^n d^3v \tag{1}$$

where $\mathbf{v}^n$ denotes the n-fold dyadic product, a tensor of rank n, and d^3v is the volume element in velocity space.

Therefore the zero-, first-, and second-order moments will be correspondingly the number density, n, the bulk flow velocity $\mathbf{V}$, and the pressure tensor $\mathbf{P}$.

It is common to use as the measurable quantity for particle counters the differential flux $j(E, \Omega)$ for particles of energy E, within a solid angle $d\Omega$. The relation between the distribution function and the differential flux is:

$$j(E, \Omega) = \frac{v^2}{m} f(\mathbf{v}) = \frac{2E}{m^2} f(\mathbf{v}) \tag{2}$$

Since $d^3v = \int d\phi \int d\theta \sin\theta \int dv v^2$ and $v = \sqrt{2E/m}$ then $d^3v = \int d\phi \int d\theta \sin\theta \int dE\sqrt{2E}/m^{3/2}$, where $d\Omega = d\phi \int d\theta \sin\theta$. Here E is the effective energy or in practice the geometric mean of a given energy channel, (for more details see chapter about phase space density), and dE is the energy width of an energy channel. Using these relations we can derive the moments as functions of measurable quantities.

B.1 Density

For the density (the zero-order moment) calculated from the 3-D data the following formula can be used:

$$n[\mathrm{cm}^{-3}] = 0.2284 \cdot 10^{-7}\sqrt{m[\mathrm{amu}]} \sum_{\phi} \Delta\phi \sum_{\theta} \Delta\theta \sin\theta \sum_{E} \frac{\Delta E[\mathrm{keV}]}{\sqrt{E[\mathrm{keV}]}} j[\mathrm{cm}^{-2}\mathrm{sr}^{-1}\mathrm{s}^{-1}\mathrm{keV}^{-1}] \tag{3}$$

In case of using omni-directional flux:

$$\sum_{\phi} \Delta\phi \sum_{\theta} \Delta\theta \sin\theta = 4\pi \tag{4}$$

Note: The central head on the ion detector is damaged therefore one can not use 3-D data for calculation of the ion number density.

B.2 Velocity

The components of the bulk flow velocity (the first-order moment) are expressed as

$$V_x[\mathrm{km\ s}^{-1}] = 10^{-5} \frac{1}{n[\mathrm{cm}^{-3}]} \sum_{\phi} \Delta\phi \cos\phi \sum_{\theta} \Delta\theta \sin^2\theta \sum_{E} \Delta E[\mathrm{keV}] j[\mathrm{cm}^{-2}\mathrm{sr}^{-1}\mathrm{s}^{-1}\mathrm{keV}^{-1}]$$

$$V_y[\mathrm{km\ s}^{-1}] = 10^{-5} \frac{1}{n[\mathrm{cm}^{-3}]} \sum_{\phi} \Delta\phi \sin\phi \sum_{\theta} \Delta\theta \sin^2\theta \sum_{E} \Delta E[\mathrm{keV}] j[\mathrm{cm}^{-2}\mathrm{sr}^{-1}\mathrm{s}^{-1}\mathrm{keV}^{-1}] \tag{5}$$

$$V_z[\mathrm{km\ s}^{-1}] = 10^{-5} \frac{1}{n[\mathrm{cm}^{-3}]} \sum_{\phi} \Delta\phi \sum_{\theta} \Delta\theta \sin\theta\cos\theta \sum_{E} \Delta E[\mathrm{keV}] j[\mathrm{cm}^{-2}\mathrm{sr}^{-1}\mathrm{s}^{-1}\mathrm{keV}^{-1}]$$

Note: For calculation of the bulk velocity the only 3-D data can be used as one needs the direction information for this. Therefore the bulk velocity can be calculated only for electrons as ions have lack of measurements in the central head.

B.3 Pressure

The diagonal terms of the kinetic pressure tensor (the second-order moment) are the following

$$P_{xx}[\text{nPa}] = 0.731 \cdot 10^{-8}\sqrt{m[\text{amu}]}\sum_{\phi}\Delta\phi\cos^2\phi\sum_{\theta}\Delta\theta\sin^3\theta\sum_{E}\Delta E[\text{keV}]\sqrt{E[\text{keV}]}j[\text{cm}^{-2}\text{sr}^{-1}\text{s}^{-1}\text{keV}^{-1}]$$

$$P_{yy}[\text{nPa}] = 0.731 \cdot 10^{-8}\sqrt{m[\text{amu}]}\sum_{\phi}\Delta\phi\sin^2\phi\sum_{\theta}\Delta\theta\sin^3\theta\sum_{E}\Delta E[\text{keV}]\sqrt{E[\text{keV}]}j[\text{cm}^{-2}\text{sr}^{-1}\text{s}^{-1}\text{keV}^{-1}]$$

$$P_{zz}[\text{nPa}] = 0.731 \cdot 10^{-8}\sqrt{m[\text{amu}]}\sum_{\phi}\Delta\phi\sum_{\theta}\Delta\theta\sin\theta\cos^2\theta\sum_{E}\Delta E[\text{keV}]\sqrt{E[\text{keV}]}j[\text{cm}^{-2}\text{sr}^{-1}\text{s}^{-1}\text{keV}^{-1}] \quad (6)$$

For the isotropic pressure

$$P[\text{nPa}] = 4\pi\frac{2}{3}0.731026 \cdot 10^{-8}\sqrt{m[\text{amu}]}\sum_{E}\Delta E[\text{keV}]\sqrt{E[\text{keV}]}j[\text{cm}^{-2}\text{sr}^{-1}\text{s}^{-1}\text{keV}^{-1}] \quad (7)$$

Note: For calculation of the pressure tensor the only 3-D electron data could be used. An isotropic pressure can be derived from both electron and ion omni-directional fluxes.

C Phase Space Density Conversion Factors

A set of fixed conversion factors between differential flux j and phase space density f based on the mean energies E_g of each channel, is listed in Table 4. More details on its calculation can be found in RAP-CR.

Chan	E_g	f/j	E_g	f/j
	Protons		Helium	
1	42.23	1.271×10^{-2}	64.18	1.338×10^{-1}
2	83.32	6.445×10^{-3}	154.0	5.576×10^{-2}
3	121.3	4.426×10^{-3}	201.2	4.269×10^{-2}
4	244.3	2.197×10^{-3}	287.2	2.991×10^{-2}
5	599.8	8.953×10^{-4}	508.6	1.689×10^{-2}
6	1340.	4.005×10^{-4}	1100.	7.806×10^{-3}
7	2748.	1.954×10^{-4}	2533.	3.392×10^{-3}
8	4007.	1.340×10^{-4}	3799.	2.261×10^{-3}
	Oxygen		Electrons	
1	151.6	9.066×10^{-1}	43.40	5.369×10^{-9}
2	337.0	4.079×10^{-1}	58.64	4.487×10^{-9}
3	454.0	3.028×10^{-1}	80.22	3.872×10^{-9}
4	563.6	2.439×10^{-1}	109.7	3.517×10^{-9}
5	777.7	1.767×10^{-1}	149.7	3.402×10^{-9}
6	1157.	1.187×10^{-1}	207.2	3.556×10^{-9}
7	1931.	7.117×10^{-2}	286.6	4.080×10^{-9}
8	3267.	4.207×10^{-2}	369.8	4.883×10^{-9}

Table 4: Conversion factors from differential flux j ($cm^{-2}s^{-1}sr^{-1}keV^{-1}$) to phase space density f ($km^{-6}s^3$). The ratio f/j is listed; to obtain f, multiple the j value by this ratio.

D RAPID to GSE Rotation Matrix

In Section 5.2, the products EFLOW_GSE and IFLOW_GSE are described, which give the GSE coordinates for each of the 9×16 (electrons) or 12×16 (ions) detector-sector combinations in the 3-D datasets, shown in Figure 2. These detectors and sectors are fixed in the spacecraft coordinate system, and must be transformed to GSE by means of the rotation matrix included in the two datasets.

Note that:

- The GSE coordinates given are the *polar* angle from the Z-axis ($0 \rightarrow 180°$) and the *azimuthal* angle from the X-axis ($-180 \rightarrow +180°$).
- The direction refers to the *flow* directions of particles detected, i.e., it is opposite to the direction in which the detector is pointing!
- The direction corresponds to the middle of each sector/detector range.

The rotation matrix alone would be sufficient to generate all the flow directions; however the results are given as a convenience to the user, and to eliminate many of the intrinsic ambiguities. A description of how to apply the rotation matrix properly is found in RAP-GSE, and a summary is given here.

D.1 The RAPID Spacecraft Frame

Let us define the RAPID coordinate system to be relative to unit vectors $\hat{u}$ along sector 0.0, $\hat{v}$ along sector 4.0, and $\hat{w}$ along the spin axis (Figure 14). The look direction for the middle of detector d in sector s has the angular coordinates

$$\theta = \pi \frac{d + 0.5}{D} \qquad \phi = 2\pi \frac{s + 0.5}{16} \tag{8}$$

where D is 12 for ions and 9 for electrons. The vector $\mathbf{L}$ for the look direction is

$$\mathbf{L} = a\hat{u} + b\hat{v} + c\hat{w} \tag{9}$$

where the cartesian coordinates are

$$\begin{aligned} a &= \sin\theta \cos\phi \\ b &= \sin\theta \sin\phi \\ c &= \cos\theta \end{aligned} \tag{10}$$

D.2 The Rotation Matrix

The 3×3 matrix for rotating from the RAPID system to GSE is given in each record of the EFLOW_GSE and IFLOW_GSE products. This matrix is determined using the following factors:

- The location of RAPID on the spacecraft (fixed!)
- The position of sector 0.0 relative to the sun pulse (has an ideal value but can vary); given in the RAPID housekeeping data.
- The GEI location of the spin axis, as given in the attitude files (varies very slowly, is updated every few days).
- The spin phase corresponding to the occurrence of the sun pulse, also in the attitude files (can vary slightly).

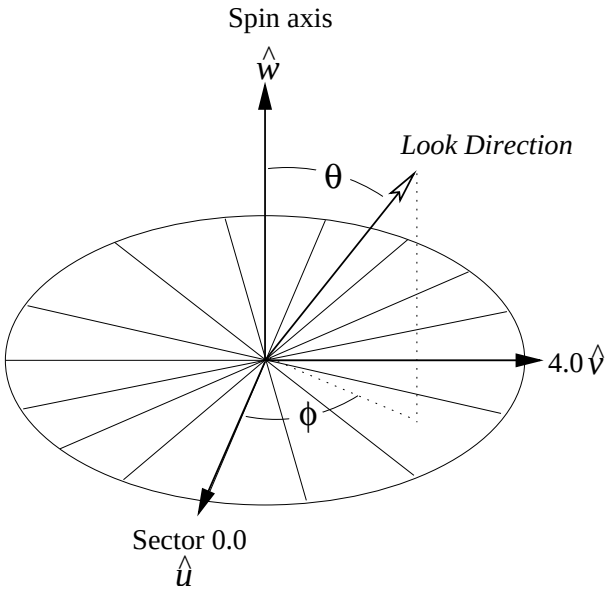

Figure 14: The RAPID spacecraft coordinate system, fixed to the spin axis ($\hat{w}$) and the start of the 16 spin sectors ($\hat{u}$). An arbitrary look direction has angular coordinates θ and ϕ.

The GEI coordinates for the spin axis are converted to GSE using standard algorithms [e.g. *Hapgood*, 1992, and references therein]. We can then determine the GSE coordinates of both the spin axis and the RAPID sector 0.0, which is sufficient to generate the rotation matrix M: its columns are simply the three vectors $\hat{u}$, $\hat{v}$, $\hat{w}$, expressed as GSE cartesian coordinates.

The flow vector $\mathbf{F}_{gse}$ is then

$$\mathbf{F}_{gse} = -\begin{pmatrix} M_{11} & M_{12} & M_{13} \\ M_{21} & M_{22} & M_{23} \\ M_{31} & M_{32} & M_{33} \end{pmatrix} \begin{pmatrix} a \\ b \\ c \end{pmatrix} \tag{11}$$

or generally,

$$\mathbf{F}_{gse} = -\mathsf{M} \cdot \mathbf{L}_{rap}$$

Note the minus sign to convert from look to flow direction!

The components of M are given in the CEF files by *row*, i.e. as M_{11}, M_{12}, ..., M_{32}, M_{33}.

D.3 Example

As an example, let us take a record from `EFLOW_GSE` for SC1 on 2001-08-22. It starts with the time stamp and the 9 values of M:

```
2001-08-22T03:30:44.501Z,
 0.49308, -0.86430, -0.09930, -0.86976, -0.49232, -0.03377, -0.01970, 0.10302, -0.99448,
```

Let us calculate the flow direction for detector 2, sector 3 (both counting from 0), which from Eqn. 8 gives us $\theta = 50°$ and $\phi = 78.75°$, and from Eqn. 10

$$a = 0.1494 \quad b = 0.7513 \quad c = 0.6428$$

We now apply Eqn. 11 to get

$$\begin{pmatrix} 0.49308 & -0.86430 & -0.09930 \\ -0.86976 & -0.49232 & -0.03377 \\ -0.01970 & 0.10302 & -0.99448 \end{pmatrix} \begin{pmatrix} -0.1494 \\ -0.7513 \\ -0.6428 \end{pmatrix} = \begin{pmatrix} 0.6395 \\ 0.5216 \\ 0.5648 \end{pmatrix}$$

The flow vector on the right is in GSE coordinates and corresponds to $\theta_{gse} = 55.61°$ and $\phi_{gse} = 39.20°$, the same values that are listed later in this record for this detector/sector combination.

```
11.69, 30.59, 50.31, 70.16, 90.04, 109.93, 129.78, 149.50, 168.38,
13.52, 32.77, 52.56, 72.44, 92.34, 112.24, 132.11, 151.85, 170.56,
14.89, 34.52, 54.41, 74.34, 94.28, 114.23, 134.14, 153.98, 172.91,
15.74, 35.64, 55.61, 75.59, 95.58, 115.56, 135.54, 155.48, 175.04,
...
77.72, 98.08, 103.33, 106.17, 108.36, 110.55, 113.39, 118.67, 139.22,
61.94, 77.07, 81.48, 83.98, 85.97, 88.02, 90.78, 96.19, 121.48,
47.09, 57.04, 60.17, 62.01, 63.52, 65.10, 67.31, 71.90, 99.59,
32.70, 37.59, 39.20, 40.17, 40.97, 41.83, 43.05, 45.71, 67.78,
...
```

D.4 Things to Note

The rotation matrices given in the two products are identical, for the same spacecraft and time. It is only the array sizes of the resulting flow matrices that are different for ions and electrons.

We have assumed here that the spin axis is identical with the body reference axis of the spacecraft. Strictly speaking, this is not true, and the attitude files also contain information on this deviation. However, these are very small ($< 0.05°$) and so have been neglected.

The rotation matrix is very nearly diagonal, meaning that its inverse (transpose) is not obviously different. This means that if one applies it in the wrong direction, a common and understandable error, the result does not appear immediately as nonesense. It is for this reason that we provide the correct results, and also emphasize how the matrix is to be filled and applied.